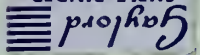


NPS ARCHIVE
1968
MERRICK, M.

A PRELIMINARY DESIGN STUDY
FOR A GROUND EFFECT MACHINE.

by

Martin Peck Merrick

 **Gaylord**
SHELF BINDER
Syracuse, N. Y.
Stockton, Calif.

UNITED STATES NAVAL POSTGRADUATE SCHOOL



THESIS

A PRELIMINARY DESIGN STUDY
FOR A GROUND EFFECT MACHINE

by

Martin Peck Merrick

March 1968

This document is subject to special export controls and each transmittal to foreign government or foreign nationals may be made only with prior approval of the U. S. Naval Postgraduate School.

LIBRARY
NAVAL POSTGRADUATE SCHOOL
MONTEREY, CALIF. 93940

A PRELIMINARY DESIGN STUDY
FOR A GROUND EFFECT MACHINE

by

Martin Peck Merrick
Lieutenant, United States Navy
B.S., United States Naval Academy, 1960



Submitted in partial fulfillment of the
requirements for the degree of
MASTER OF SCIENCE IN AERONAUTICAL ENGINEERING
from the
NAVAL POSTGRADUATE SCHOOL
March 1968

1968

MERRICK, M.

~~1/23/5
M 35
cr 1~~

ABSTRACT

This paper provides the results of a preliminary design study of a ground effect machine to be built at the Naval Postgraduate School, Monterey, California. The design is based on an engine currently available at the School and covers such factors as lift versus weight, thrust versus drag, balance, stability, control, and instrumentation. The final design chosen was a peripheral jet type ground effect machine with a cushion area of 25.7 square feet, driven by a 4 foot diameter shrouded propeller. Total engine power of 203 horsepower is sufficient to provide 1017 pounds of lift at a hover height of 5.95 inches and 446 pounds of thrust at 30 knots.

TABLE OF CONTENTS

CHAPTER	PAGE
LIST OF TABLES	5
LIST OF FIGURES.	7
LIST OF COEFFICIENTS AND SYMBOLS	9
I. INTRODUCTION	17
II. GENERAL THEORY	18
III. POWER PLANT	20
IV. VEHICLE PHYSICAL CHARACTERISTICS	22
V. PROPELLER SELECTION	25
VI. LIFT POWER AVAILABLE	26
VII. DRAG AND PROPULSIVE POWER	31
VIII. CONTROL	33
IX. INSTRUMENTATION	38
X. CONCLUSIONS	39
BIBLIOGRAPHY	60
REFERENCES	62
APPENDIX A	63
APPENDIX B	65

LIST OF TABLES

TABLE	PAGE
I. Leading Particulars	40
II. Vehicle Dimensions	42
III. Structural Weights, Airframe	43
IV. Weights of Other Structural Members and Accessories	44
V. Estimated Pitching Moments	45
VI. Propeller Performance Estimation	46
VII. Propeller Selection Criteria	48
VIII. Yaw Control Data	49
IX. Pitch Control Data	50
X. Throttling Altered Parameters	51

LIST OF FIGURES

FIGURE	PAGE
1. Bleed Air Ducting Including Converging-Diverging Nozzle	52
2. Left Side View of Ground Effect Machine, Final Design	53
3. Top View of Ground Effect Machine, Final Design	54
4. Front View of Ground Effect Machine, Final Design	55
5. Rudder Control Moment vs. Rudder Deflection Angle	56
6. Elevator Control Moment vs. Elevator Deflection Angle	57
7. Throttle Mechanism	58
8. Orientation of Θ , t and h	59

LIST OF COEFFICIENTS AND SYMBOLS

A_i	Area of compressor bleed air outlet
A_2	Air flow area at the propeller plane = $(\pi/4 D_p^2)(1 - CB_2^2) = .714 D_p^2$, square feet
A_4	Air flow area at the shroud exit plane = $(\pi/4 D_4^2)(1 - CB_4^2)$, square feet
b	Cushion beam, feet
b	Blade section width, feet - (propeller selection)
B	Number of propeller blades
BHP	Shaft brake horsepower
C	Cushion perimeter, feet; Mass ratio, Appendix B
CB_2	Centerbody size at propeller plane, fraction of propeller diameter = 0.30
CB_4	Centerbody size at shroud exit plane, fraction of shroud exit diameter
C_{De}	External aerodynamic drag coefficient ($D_e/q_a S$)
C_L	External aerodynamic lift coefficient ($L/q_a S$)
C_{Ld}	Blade section design lift coefficient
C_{Li}	Integrated design lift coefficient = $4 \int_{.3}^{1.0} C_{Ld} x^3 dx$
C_j	Jet reaction coefficient
C_{Lr}	Three dimensional lift coefficient, rudder
C_{Le}	Three dimensional lift coefficient, elevator
C_p	Power coefficient = $\frac{P}{\rho_0 n^3 D_p^5} = \frac{\text{BHP} (\rho_{sl}/\rho_0)}{2000 (.1/1000)^3 (D_p/10)^5}$
c_l	Two dimensional (section lift coefficient)
D_e	External aerodynamic drag, pounds
D_p	Propeller diameter, feet

D_r	Ram or momentum drag, lb.
D_T	Total drag, lb.
D_4	Duct diameter at shroud exit plane, feet
f_c	Ratio of speed of sound at standard day level to the speed of sound at the operating condition
F_D	Shroud drag loss factor
g	Acceleration due to gravity, feet/second ²
G.R.	Gear ratio, propeller speed/engine speed
h	"Daylight" gap, feet (local value or mean value as appropriate)
J_o	Propeller advance ratio based upon vehicle velocity = $101.4 V_{ok}/ND_p$
J_2	Propeller advance ratio based upon duct velocity = $101.4 V_{2k}/ND_p$
J_{2ideal}	Propeller advance ratio based upon duct velocity determined under ideal flow conditions
J_{2max}	Maximum J_2 to avoid compressibility losses
l	Cushion length, feet
L	Total lift, pounds
L_e	External aerodynamic lift, pounds
\dot{m}_i	Mass flow rate out of compressor, pounds/minute
\dot{m}_N	Mass flow rate out of nozzle, pounds/minute
M_o	Vehicle Mach number = $V_{ok} \cdot f_c / 662$
M	Control moment, pitch, foot-pounds
N	Control moment, yaw, foot-pounds
N	Propeller speed, revolutions per minute (propeller selection)

P_c	Total shaft power supplied to cushion system, pound-feet/second
P_L	Lift horsepower, horsepower
P_p	Total shaft power supplied to propulsion system, pound-feet/second
P	Total shaft power ($P_c + P_p$), pound-feet/second
P_a	Atmospheric pressure, pounds/foot ²
P_i	Pressure at compressor bleed air outlet, pound/foot ²
P_N	Static pressure at nozzle, pound/foot ²
P_t	Total pressure of air supply to cushion at nozzle exit or cushion entry, pounds/foot ²
q	Local dynamic pressure ($\rho u^2/2$), pounds/foot ²
q_a	Reference air dynamic pressure ($\rho_a V_o^2/2$), pounds/foot ²
Q	Total air volume flow rate through cushion system, foot ³ /second
r_p	Radius at blade element, feet
R	Gas constant for air, feet/degree Fahrenheit
R	Blade radius at propeller tip, feet
AR	Aspect ratio
S_g	Daylight gap area (cushion perimeter times mean daylight gap, hC , feet ²)
S_N	Total nozzle area, feet ²
S	Cushion area, feet ² , measured, in plan view, to outer edge of nozzle exit
t	Nozzle thickness, feet
T_i	Air temperature at compressor bleed air outlet, degrees Rankine

T_N	Air temperature at nozzle, degrees Rankine
T_p	Propeller thrust, pounds
T_T	Total thrust, uncorrected for shroud drag loss, pounds
T_{TE}	Total thrust, corrected for shroud drag loss, pounds
T_{Pideal}	Propeller thrust, determined for ideal flow conditions, pounds
T_{Tideal}	Total thrust, determined for ideal flow conditions, pounds, for T_T , T_{TE} , T_{Pideal} , and T_{Tideal}
	for $V_{ok} > 0$, $T = \frac{326 \text{ BHP } \eta_o}{V_{ok}}$
	where the subscript on η_o is the same as the subscript on T
	for $V_{ok} = 0$, $T = C_T/C_p \cdot \text{BHP}/ND_p \cdot 33000$
	where the subscript on C_T/C_p is the same as the subscript on T
TAF	Total blade activity factor = $100000/16 B \int_{.3}^{1.0} (b/D_p) X^3 dX$
u	Local air velocity, feet/second
V_i	Velocity of air flow out of compressor, feet/second
V_c	Cushion reference velocity ($\sqrt{2/\rho \Delta p}$), feet/second
V_j	Jet velocity of air discharge from GEM base, when fully contracted, feet/second
V_{ok}	Vehicle velocity, knots
V_{2k}	Duct velocity at the propeller plane, knots
$V_{2kideal}$	Duct velocity at the propeller plane determined for ideal flow conditions, knots
\dot{w}	Volume flow rate out of compressor, ft ³ /min
w	Cushion loading (W/S), lb/ft ²

W	Gross weight of vehicle, lb
x	Nozzle thickness parameter $\left[\frac{t}{h(1 + \sin \Theta)} \right]$
X	Fraction of propeller tip radius, r_p/R
α_{or}	Rudder deflection angle, degrees
α_{oe}	Elevator deflection angle, degrees
α_{er}	Effective angle of attack, rudder, degrees
α_{ee}	Effective angle of attack, elevator, degrees
α_{ir}	Induced angle of attack, rudder, degrees
α_{ie}	Induced angle of attack, elevator, degrees
\mathcal{D}_c	Cushion discharge coefficient $\frac{Q}{c_p \sqrt{2\rho \Delta p}}$
η_{oP}	Propeller efficiency based on vehicle velocity
η_{oT}	Total efficiency (shroud and propeller) based upon vehicle velocity, uncorrected for shroud drag loss
η_{oTE}	Total efficiency (shroud and propeller) based upon vehicle velocity, corrected for shroud drag loss
	$\eta_{oT}^{XF_D}$
$\eta_{oP_{ideal}}$	Propeller efficiency based upon vehicle velocity for ideal flow conditions
$\eta_{oT_{ideal}}$	Total efficiency (shroud and propeller) based on vehicle velocity for ideal flow conditions
η_{2P}	Propeller efficiency based on the duct velocity approaching the propeller plane
$\eta_{2P_{ideal}}$	Propeller efficiency based upon the duct velocity approaching the propeller plane for ideal flow conditions
$\Theta_{3/4}$	Propeller blade angle at $X = 3/4$, degrees
Θ	Peripheral jet efflux angle

γ_i	Specific weight of air at compressor bleed air/outlet, pounds/foot ³
γ_N	Specific weight of air at nozzle, pounds/foot ³
γ_a	Specific weight of air at compressor inlet, pounds/foot ³
ρ_0	Mass density of air, slugs per cubic foot
ρ_N	Air density at nozzle, slugs/foot ³
Δp	Cushion pressure, psfa
ζ	Induced angle of attack correction for nonelliptic lift distribution
δ	Induced drag correction for nonelliptic lift distribution

SUBSCRIPTS

o	Represents free stream conditions
2	Represents conditions and duct geometry just upstream of the propeller plane
2	Conditions at exit of converging-diverging nozzle
3	Conditions at exit from large duct (entrance to peripheral nozzle system)
4	Represents conditions and duct geometry at the shroud exit plane
E	Represents performance values corrected for shroud drag losses
b	Section between converging-diverging nozzle exit and large duct (bypass conditions)
k	Knots
P	Represents the propeller only within the shroud
T	Represents total quantities (shroud and propeller)
SL	Represents sea level standard day conditions
oP	Represents propeller performance relative to the free stream
oT	Represents total (shroud and propeller) performance relative to the free stream, but uncorrected for shroud drag losses
oTE	Represents total (shroud and propeller) performance relative to the free stream, corrected for shroud drag losses
o2	Stagnation conditions at station 2
o3	Stagnation conditions at station 3

CHAPTER I

INTRODUCTION

This project was undertaken to investigate the feasibility of building a ground effect machine utilizing an engine currently available, the AiResearch Pneumatic and Shaft Power Gas Turbine Engine Model GTCP 85-91. This engine supplies pneumatic power in the form of compressed bleed air and simultaneously, or independently, supplies a source of constant speed shaft power. In this installation the pneumatic power will be utilized to provide lift power while the shaft power will be used to drive a propeller to provide propulsive power.

Several different basic designs were considered with the finding that only two, the open plenum and the annular jet, were simple enough and had enough information readily available to make them convenient for study. Once a particular type machine had been chosen, the amount of power available from the engine could be used to calculate the weight and ultimately the size of the vehicle which could be built. Consideration was given only to a relatively small vehicle with limited performance characteristics. This was due to the limited power available from the engine as well as the vehicle's designed use, an experimental vehicle useful in the course of instruction in Aeronautical Engineering at the Naval Postgraduate School.

While it is realized that flexible skirts and fingers could provide a considerable increase in overall efficiency, they were not included in this design because they would not have been in keeping with the basic simple design desired. Also, skirts have been shown (Ref. 1) to create maintenance problems and costs out of proportion with the vehicle's design use.

CHAPTER II
GENERAL THEORY

Of the several ground cushion concepts being studied in the United States, the author decided to utilize the simple air curtain or peripheral jet concept. As in all ground cushion concepts, the major source of lift is the ground cushion itself, a region of positive pressure trapped between the base of the vehicle and the ground. In the simple air curtain vehicle, the ground cushion is produced and contained by air exhausted downward and inward from a nozzle at the periphery of the base.

2.1 Hovering

The contribution to lift of the jet reaction force is small compared to the cushion lift. The lift is thus approximated by the product of cushion pressure times base area.

$$L = \Delta p S$$

Also the cushion pressure reacts against the air curtain sufficiently to balance the momentum change within the curtain, that is

$$\Delta p_{th} = \rho N_j^2 t (1 + \sin \Theta) \quad (\text{See Appendix A.}) \quad (\text{II-1})$$

Hovering performance can be expressed by a dimensionless figure of merit

$$M = (1 + \sin \Theta) \frac{\sqrt{t/n (1 + \sin \Theta)}}{1 + t/n (1 + \sin \Theta)} - \frac{S}{nC}$$

which will allow the vehicle to be compared with the performance of the ideal shrouded propeller or helicopters. M will have a maximum value (when $t/n = 1/2$, $\Theta = 90^\circ$) of

$$M_{opt} = 1 - \frac{S}{nC}$$

The ratio S/hC , called the size/height ratio, is important in "virtually all considerations of all types of ground effect machines" (Ref. 2).

2.2 Cruise

In forward flight there will be two modifications to the hovering equations. First, the propulsion system must expend energy at the rate

$$P_p = D_{ram} V_o$$

to overcome ram drag, a force equal to the air mass flow rate through the peripheral nozzle times the vehicle forward velocity. Second, the required pressure rise through the compressor is reduced by q_o , the free stream dynamic pressure recovered by the inlet.

Cruise performance is frequently expressed by the "equivalent lift/drag ratio," $\frac{LV_o}{P}$, to which both range and operating cost per mile are directly related. The optimum value of $\frac{LV_o}{P}$ for $t/h = \left(\frac{1}{2} + \frac{1}{1 + \nu^2}\right)$

and $\Theta = 90^\circ$ is

$$\frac{LV_o}{P} = 2 \frac{S}{hc} \frac{\nu}{\sqrt{1 + \nu^2}}$$

where

$$\nu = V_o \sqrt{L/\rho_N S}$$

Limiting values of equivalent lift/drag ratio of about $0.7 \frac{S}{hC}$ are expected for practical vehicles.

CHAPTER III

POWER PLANT

The pneumatic and shaft power gas turbine engine Model Number GTCP 85-91 is built by the Garrett Corporation, AiResearch Manufacturing Division, Phoenix, Arizona, and was originally designed to supply pneumatic power in the form of compressed bleed air for the operation of aircraft main engine starters and simultaneously, or independently, to provide a source of constant speed shaft power for driving an alternator or other shaft driven equipment. Use of this unit as the main power supply for a ground effect machine (GEM) alters its output use considerably. The pneumatic power output will in this case be used to provide lift for the GEM. Simultaneously, the shaft output will be used to drive a shrouded propeller providing thrust for forward flight as well as a flow of air over the primary control surfaces.

The unit is basically composed of a two-stage centrifugal compressor assembly directly coupled to a radial inward-flow turbine wheel. The rotating shaft power of the turbine in excess of that required to drive the compressor is absorbed by the accessory output shaft, compressor and accessories.

Operation and a complete description of the engine itself are described in Ref. 3 (Operation and Maintenance Instructions). Reference 3 also lists the leading particulars concerning the engine, the most important of which are reproduced in Table I.

The actual power available for lift was computed as follows:

$$\text{Power} = (\text{volume flow rate})(\text{pressure rise})$$

that is

$$\text{HP}_{\text{avail}} = \frac{\dot{m}}{\gamma_a} (p_{\text{out}} - p_{\text{in}})$$

where \dot{m} and p_{out} are from Table I for pure bleed loan condition, and ρ_a and p_{in} are based on NACA Standard Sea Level Day conditions. This calculation revealed a maximum of 203 horsepower available for lift.

Due to the particular conditions at the compressor bleed air outlet (high pressure, high temperature, and low velocity) it is necessary to find some way to convert this energy to a more useable form. It is proposed to accomplish this by using a jet pump such as is shown in Fig. 1. The purpose of this apparatus is to use the high pressure air source as a "pump" in order to achieve an increased flow rate and velocity out of the vehicle's peripheral nozzle. This is accomplished by first accelerating the air to supersonic velocity using a converging-diverging nozzle. This high velocity air is then ejected into a larger area pipe which has the effect, through viscous interaction, of increasing the mass flow rate by the amount of atmospheric air entering the large pipe. The two streams mix and are then ducted at constant area into the vehicle's peripheral jet system.

CHAPTER IV

VEHICLE PHYSICAL CHARACTERISTICS

Reference 4 indicates that, in general, approximately one-half of the total power required will be utilized for lift. Thus based on the above power available, as an initial approximation we can assume 100 horsepower available for lift. Chaplin's theory as quoted in Chapter 2 of Ref. 4 indicates

$$P_L = \frac{W}{2\sqrt{\rho}} \sqrt{W/S}$$

P_L = lift horsepower

W = vehicle gross weight

W/S = vehicle planform loading

ρ = density of air

Assuming $W/S = 35$, a value typical for vehicles in the small category, we can solve the above equation for weight using the power available for lift.

$$W = \frac{2\sqrt{\rho} P_{avail}}{\sqrt{W/S}} = 900 \text{ lbs}$$

Thus the available power plant should provide sufficient lift and thrust for a vehicle weighing approximately 900 pounds.

4.1 GEM Type and Shape

References 2, 4, 5, and 6 indicated that the peripheral-jet GEM is more efficient than the plenum chamber type machine. For that reason, all further considerations were given to that type machine. Reference 5 indicates that the best thrust augmentation is obtained with a machine having a circular planform, but the loss in augmentation resulting from the use of an elongated planform does not become very

large until the ratio of length to width becomes greater than three. Therefore, to simplify construction as well as stability and control considerations which will be discussed later, an elongated planform with length to beam ratio = 2 was chosen. Initial consideration was given to an elliptical planform, but the final shape as shown in Figs. 2, 3, and 4 was chosen to avoid double curvature in construction and to simplify construction of control surfaces. Table II lists the basic dimensions of the GEM as well as some of the other important parameters which will be used in the subsequent analysis of the vehicle's performance.

4.2 Weight

Before an accurate analysis of performance can be made, knowledge of the vehicle's weight must be available.

Reference 4 suggests that the hull be constructed of 0,028 inch aluminum which provides adequate structural strength as well as response to impacts. Table III shows various portions of the structure and their associated weights. Table IV indicates the weight of other structural members as well as all other associated equipment and accessories. The weight of electrical wiring was assumed to be negligibly small. The total weight of the GEM is 1017 pounds.

4.3 Physical Arrangement

The location of the various components and accessories in the final design was somewhat arbitrary, keeping in mind, however, balance of the vehicle and general considerations such as pilot's visibility, etc.

4.4 Balance

With regard to balance, all major components are located either on or symmetrically about the vehicle's roll axis. Therefore only

pitching moments due to component placement were considered. Table V shows the estimated pitching moments created by the major components.

CHAPTER V

PROPELLER SELECTION

Selection of a propeller to be used for vehicle propulsion and to provide a continuous flow of air over the control surfaces was based on Ref. 7, one of the famous "Red, White and Blue Books." Various combinations of propeller speed, total activity factor, diameter, and integrated design lift coefficient were considered. In order to not have the propeller extend beyond the vehicle edges, it was decided to limit the diameter to 4 feet.

Calculations were made for vehicle velocities of zero (hover), 20 knots and 30 knots. Final selection was based on the estimated value of η_{2p} , propeller efficiency based on V_2 . A tradeoff was made between the best efficiencies under various flight regimes. Table VI shows the final six possible propellers with the ultimate selection being 600 TAF, $0.5C_{Li}$, and 2700 RPM.

Since the engine shaft output is at a constant 6000 RPM, the propeller selected requires a 20:9 gear reduction. This is accomplished by a two gear train mounted between the engine and the propeller itself.

Weight of the propeller and reduction gears was estimated to be 150 pounds (solid steel construction, 0.3 ft^3 at 389.6 lb/ft^3).

After the propeller had been selected, calculations were made at various power settings and vehicle velocities to obtain values of thrust available for comparison with drag as calculated in Chapter VII. These calculations are shown in Table V.

CHAPTER VI

LIFT POWER AVAILABLE

Assuming that the power available from the compressor is split with 50 per cent utilized for lift and 50 per cent for thrust (propulsion), the lift power and actual lift can be found as follows.

From the engine specifications, one-half of the pneumatic power out is 65.25 pounds/minute at 95 inches Hg absolute. The velocity of the air flow at the compressor outlet can be found from the continuity equation,

$$\gamma_{AV} = \dot{m} = \text{constant}$$

Assuming a perfect gas relation,

$$\gamma_i = \frac{p_i}{RT_i}$$

where

$$\gamma_i = \text{specific weight of air at the compressor bleed air outlet}$$

$$p_i = \text{pressure at the compressor bleed air outlet}$$

$$= (95)(70.7)$$

$$= 6710 \text{ lb/ft}^2$$

$$T_i = \text{temperature at compressor bleed air outlet}$$

$$= 943^\circ\text{R}$$

$$\gamma_i = \frac{6710}{53.3(943)}$$

$$= 0.1335 \text{ lb/ft}^3$$

At the compressor outlet then

$$V_i = \frac{\dot{m}}{\gamma_i A_i}$$

$$= \frac{56.25}{.1335(.0716)(60)}$$

$$V_i = 98.1 \text{ ft/sec}$$

Utilizing isentropic flow tables from Ref. 8 and a nozzle exit pressure of 1058.4 psf (0.5 atm), the conditions at station 2, the nozzle exit, can be found. This nozzle exit pressure was found using an iterative process as described in Appendix B. With this value of nozzle exit pressure, the computed value of X, the mass flow rate ratio, is

$$X = 20.09$$

which yields the following:

$$\begin{aligned} \dot{m}_b &= (X)(\dot{m}_2) \\ &= 20.09(.0299) \\ &= 0.6006 \text{ slug/sec} \end{aligned}$$

$$\begin{aligned} \dot{m}_3 &= \dot{m}_b + \dot{m}_2 \\ &= .6006 + .0299 \\ &= .6305 \text{ slug/sec} \end{aligned}$$

$$\begin{aligned} V_b &= X/C \\ &= 20.09/.0181 \\ &= 1109 \text{ ft/sec} \end{aligned}$$

$$\begin{aligned} T_3 &= (T_2 + XT_b)/(X + 1) \\ &= 555 + 426(20.09)/21.09 \\ &= 432^\circ\text{R} \end{aligned}$$

$$\begin{aligned} V_3 &= (V_2 + XV_b)/(1 + X) \\ &= [2159 + 20.09(1110)]/21.09 \\ &= 1159 \text{ ft/sec} \end{aligned}$$

$$\begin{aligned} p_3 &= \dot{m}_2(1 + X)(gRT_3)/A_3V_3 \\ &= .0299(21.09)(32.2)(53.3)(432)/(.4)(1159) \\ &= 1008 \text{ psf} \end{aligned}$$

$$\begin{aligned}\rho_3 &= p_3 / gRT_3 \\ &= 1008 / (32.2)(53.3)(432)\end{aligned}$$

$$\rho_3 = 0.001359 \text{ slugs/ft}^3$$

$$\begin{aligned}M_3 &= V_3 / 49.0179 \sqrt{T_3} \\ &= 1159 / 49.0179 \sqrt{432} \\ &= 1.1375\end{aligned}$$

Once again assuming isentropic conditions, the stagnation values at station 3 can be found.

$$p_{o3} = 2260 \text{ psf}$$

$$\rho_{o3} = 0.002418 \text{ slugs/ft}^3$$

$$T_{o3} = 544^\circ\text{R}$$

$$A_{3}^* = 0.3941 \text{ ft}^2$$

Since it is known that the peripheral nozzle exit pressure, p_N , must be atmospheric, the exit Mach number, M_j , can be found from

$$\begin{aligned}\frac{p_N}{p_{oN}} &= \frac{2116.8}{2260} \\ &= 0.9366\end{aligned}$$

This yields

$$M_j = 0.31$$

$$p_N / p_{oN} = 0.9535$$

$$T_N / T_{oN} = 0.98114$$

$$S_N / A_N^* = 1.976$$

from which the static nozzle values of density, temperature and area can be found.

$$\rho_N = 0.002305 \text{ slugs/ft}^3$$

$$T_N = 534^\circ\text{R}$$

$$S_N = 0.779 \text{ ft}^2$$

Now the jet velocity, V_j , can be found from

$$\begin{aligned} V_j &= M_j(41.0179) \sqrt{T_N} \\ &= 0.31(49.0179) \sqrt{534} \\ &= 351 \text{ ft/sec} \end{aligned}$$

Since the nozzle area, S_N , is the product of the cushion perimeter, C , and the nozzle thickness, t , the necessary thickness can be found.

$$\begin{aligned} t &= S_N/C \\ &= (12 \text{ in/ft})(0.779)/20.5 \\ &= 0.456 \text{ in.} \end{aligned}$$

Next the lift, L , acting on the GEM can be found from

$$L = \Delta p S + (C_j - 1) \Delta p S_N \cos \theta + C_L q_a S$$

where

$$\begin{aligned} S &= \text{cushion area} \\ &= 25.7 \text{ ft}^2 \end{aligned}$$

and C_j is shown (Ref. 6) to be

$$C_j = \frac{1}{1 - e^{-2x}} + \frac{1}{2x}$$

The last term in the lift equation is zero for hover conditions and will be relatively small for any operating condition.

For equilibrium conditions, lift must equal the weight of the vehicle. Making use of these two facts and the definition of x and substituting equation II-1 into the above lift equation yields

$$W = \rho_N V_j^2 x S + \left[\frac{1}{1 - e^{-2x}} + \frac{1}{2x} - 1 \right] \rho_N V_j^2 x S_N \cos \theta$$

which can be solved numerically for x .

$$x = 0.115$$

This value leads to

$$\begin{aligned}h &= (t/x)(1 + \sin \theta) \\ &= (.456/.115)(1.5) \\ &= 5.95 \text{ in.}\end{aligned}$$

The above analysis was "ideal" in many ways. Changes in weight or engine power will be manifested in changes in hover height, h . For example, a change in weight to 1200 lb. can be shown to change the hover height to 4.79 in.

Similarly, a change in engine power will create a complex change in the lift equation due to the fact that the cushion peripheral nozzle will no longer be operating under design conditions (non-optimum pressure). This will, however, result only in a change in hover height. For example, a 10 per cent decrease in the product $\rho_N V_j^2$ will decrease hover height by 0.68 in. Thus the GEM will continue to operate satisfactorily under off-design conditions.

CHAPTER VII

DRAG AND PROPULSIVE POWER

The external aerodynamic drag of the vehicle can be calculated as follows:

$$D_e = C_{De} S q_a$$

where

D_e = external drag

C_{De} = external drag coefficient--assumed worst conditions; i.e., flat plate (Ref. 9)

S = cushion base area = 25.7 ft²

$$\begin{aligned} D_e &= (1.28)(25.7)(1/2 \rho_a V_o^2) \\ &= 100.5 \text{ lb.} \end{aligned}$$

The symbol q_a is as previously defined.

The only other applicable source of drag is ram or momentum drag which arises from bringing a constant mass flow rate of air \dot{m} from a velocity V relative to the GEM to a zero velocity relative to the GEM. Thus,

$$D_r = \dot{m}V = \rho_N V_j (D_c S_g) V_o$$

where

D_c = discharge coefficient, cushion (Ref. 9)

and

S_g = daylight gap area

D_c may be found from

$$D_c = \bar{D}_c \sqrt{\frac{\tanh \frac{x}{2}}{[\bar{D}_c (1 + \sin \theta)]^2}}$$

where

$$\begin{aligned} \bar{D}_c &= 1/2 \left[1 + \frac{\cos \theta}{\frac{\pi + 2}{\pi - 2} (1 + \sin \theta) - \sin \theta \cos \theta} \right] \\ &= 0.5685 \end{aligned}$$

Thus

$$D_c = 0.327$$

Ram drag, D_R , is thus found to be

$$\begin{aligned} D_R &= (.002305)(351)(.327)(10.17)(30)(6080/3600) \\ &= 134 \text{ lb.} \end{aligned}$$

Total drag which equals the sum of ram drag and external aerodynamic drag is thus found to be

$$\begin{aligned} D &= D_R + D_e \\ &= 134 + 100.5 \\ &= 234.5 \end{aligned}$$

It is felt that the external drag coefficient will probably be much smaller than the value assumed above. The total drag will thus be smaller also. However, even at these "worst" conditions, computed drag is much less than thrust available. The drag of the propeller shroud is not considered in the above analysis due to its being accounted for in the analysis of propeller/shroud combination to obtain thrust available.

CHAPTER VIII

CONTROL

Control of the vehicle is accomplished through the use of a single rudder, two elevators and nozzle throttling within the peripheral jets. The control surfaces are activated by the pilot's rudder pedals and control column.

8.1 Yaw

Control in yaw is effected by the use of a single aircraft type rudder actuated by the pilot's rudder pedals. A symmetrical airfoil section, the NACA 0009, was chosen both for simplicity and to have zero force in the neutral position. Data for this airfoil were taken from Ref. 7 and tabulated in Table VII. Note that two dimensional data are converted to three dimensions by computing an effective angle of attack as indicated in Chapter 5 of Ref. 7. Figure 5 is a plot of rudder control moment vs. rudder deflection.

8.1.1 Sample Yaw Control Calculation

Control analysis (yaw)

$$b = 4 \text{ ft.}$$

$$c = 1 \text{ ft.}$$

$$S = bc = 4 \text{ ft}^2$$

$$AR = \frac{b^2}{S} = 4$$

For an unswept, zero taper airfoil, from Fig. 5:4, Ref. 7, for $c_t/c_r = 1.0$

$$\tau = 0.166$$

$$\delta = 0.05$$

$$\text{mass flow in unit time} = \rho_o S^{\dagger} V_4$$

where

$$V_4 = (A_2/A_4)V_2(6080/3600)$$

$$= (1/1.2)(96.9)(6080/3600)$$

$$= 136.377 \text{ ft/sec}$$

Also for the given conditions, the Reynolds number is given by

$$Re = \frac{\rho V d}{\mu}$$

or

$$\frac{Re}{\lambda} = \frac{a}{\gamma} \cdot M$$

$$= \frac{a}{\gamma} \frac{V_4 k}{662}$$

$$= 0.871 \times 10^6$$

Thus from Ref. 7, at $\alpha_0 = 10^\circ$, $c_1 = 1.05$ and

$$L = 1/2 \rho V^2 c_1 S$$

$$= (.5)(.002378)(136.377)^2(1.05)(4)$$

$$= 92.878 \text{ lb.}$$

Thus

$$\alpha_i = \frac{2L}{\rho \pi b^2 V^2}$$

$$= 0.0836 \text{ radians (uncorrected)}$$

$$\alpha_i \text{ (corrected)} = \alpha_i (1 + \zeta)$$

$$= 0.0975 \text{ radians}$$

$$= 5.58^\circ$$

Then

$$\alpha = \alpha_0 - \alpha_i$$

$$= 10 - 5.58$$

$$= 4.42^\circ$$

Therefore

$$C_{1r} = 0.45$$

and

$$\begin{aligned}L_r &= (1/2) \rho v^2 C_{l_r} S \\ &= 39.805 \text{ lb}\end{aligned}$$

Assuming the point of action of lift to be at $0.25c$, the force acts at 3.5 feet from the vehicle's center of gravity. Thus a control moment, N , can be found.

$$N = L_r l_r$$

where

$$l_r = \text{distance from a.c. (rudder) to} \\ \text{c.g. (vehicle)}$$

Thus

$$\begin{aligned}N &= (39.805)(3.5) \\ &= 139.317 \text{ ft-lb}\end{aligned}$$

8.1.2 Yaw Control Results

Since the vehicle rides on an air cushion and will travel only at very low velocities, there will be little force to oppose the motion created by the rudder force. Thus the small moment available will be entirely sufficient for directional control. It is also important to note that this same phenomenon, that is little opposing force, will necessitate the pilot's physically stopping a turn by applying a rudder force in the opposite direction.

8.2 Pitch

Analysis of the vehicle's pitch control is similar to the above analysis of yaw control. The airfoil section selected for the elevators is the same as that used for the rudder. Thus the only difference will result from the elevator's being split into two sections, each with smaller span than one half the rudder.

Since the elevators are placed symmetrically about the vehicle centerline, there should be no rolling moment created by their being split. With this in mind, only pitch reaction to the elevators will be studied.

It was immediately noted that the use of one-foot chord for the elevators allowed the possibility of control reversal at some deflection angles due to three dimensional effects. This problem was eliminated by choosing a 0.5 foot chord length for the elevators.

8.2.1 Pitch Control Sample Calculation

Look now at a NACA 0009 airfoil with span 21.5 inches and chord 0.5 feet:

$$\begin{aligned}b_e &= 21.5/12 \\ &= 1.79 \text{ ft} \\ c_e &= 0.5 \text{ ft} \\ S_e &= b_e c_e \\ &= 0.895 \text{ ft}^2\end{aligned}$$

Thus it has aspect ratio:

$$\begin{aligned}AR &= b^2/S \\ &= 3.58\end{aligned}$$

Once again the airfoil is unswept and untapered so that

$$\begin{aligned}\gamma &= 0.166 \\ \delta &= 0.05\end{aligned}$$

8.2.2 Pitch Control Results

Table VIII contains airfoil data for the elevators as well as the results of pitch control analysis. Note that as was the case with rudder control, the pitch control moment is positive at all elevator deflections. Figure 6 is a plot of pitch control moment vs. elevator deflection angle. The magnitudes of the pitch control moments are

acceptable but only marginally so. For instance, a 20 pound change in the predicted weight of the pilot would require almost full elevator deflection to maintain level flight. Thus a set of nozzle throttles as discussed in Section 8.3 might be in order if a great deal of flexibility is desired.

8.3 Roll Control

Control in roll is achieved through the use of throttles within the side portions of the jet nozzles. Figure 7 is an actual side view of the general arrangement used. Actuation of the throttle on either side is by means of the pilot's control stick. The result of throttle actuation is to reduce nozzle thickness, t , and jet efflux angle, Θ , over a portion (one side) of the periphery. This has the effect of altering several of the vehicle's characteristic performance parameters. Table IX is a summary of these changes. The total lift now becomes

$$L = \Delta p' S + (C_j - 1) \Delta p' (.805 S_N) \cos \Theta \\ + (C_j - 1) \Delta p' (t') (.195 C) \cos \Theta'$$

where the third and second terms on the right hand side of the equation account for the jet reaction over the throttled portion and the remainder of the nozzle area respectively. The rolling moment produced will be the result of the difference between the jet reaction of the throttled and unthrottled sides of the vehicle. Over the 4 foot unthrottled side section, the jet reaction force is 66.4 pounds while on the throttled side, the reaction force is 44.9 pounds. Thus a rolling moment about the vehicle centerline of 86 foot-pounds is produced.

CHAPTER IX
INSTRUMENTATION

Very little instrumentation will be required on the vehicle. At the modest performance characteristics expected, little or no help from instruments will be needed to "fly" the machine. A minimum number of engine monitoring instruments are of course necessary to insure that the engine's limitations are not exceeded.

If at some future period it is desired to thoroughly instrument the vehicle for the purpose of performance evaluation, there should be no problems encountered with regard to either weight or power to run the instruments. However, since the vehicle is quite small, some problems would probably be encountered in trying to find space available to mount the instruments.

CHAPTER X

CONCLUSIONS

The design and building of a small ground effect machine at the Naval Postgraduate School is without doubt a feasible project. Utilization of the AiResearch GTCP 85-91 for both lift and propulsion power is well within the realm of possibility. The amount of power available is somewhat greater than that required by the roughly 1000 pound vehicle which was designed in this paper.

It is felt, however, that this was not the most practical avenue of approach to the design problem. Rather, the establishment of some performance criteria followed by the selection of a machine, engine, and propeller combination to meet those criteria would be a more realistic problem.

TABLE I
LEADING PARTICULARS

Turbine Section

Wheel Governed Speed (no-load).....41,200 +0 RPM
-100

Discharge Temperature

Steady-state Full-load Condition.....628°C (1165°F) (MAX)

Compressor Section

Inlet Temperature.....54°C (130°F) (MAX)

Discharge Temperature

Steady-state Condition with 54°C (130°F)

Inlet Air Temperature.....250°C (483°F) (MAX)

Accessory Section

Output Shaft Speeds

Alternator.....6000 RPM (APPROX)

Output Ratings

Pure Shaft Load.....182 HP (MAX)

Pure Bleed Load.....(NACA STD SL DAY), 112.5 lbm per
MIN at 95.0 IN. HG Abs (Static)

Fuel and Fuel Control System

Fuel Specification.....MIL-F-5624, Grade JP3 and JP4; MIL-F-5572
and ASTM Type A and B

Recommended Fuel Boost Pump Setting.....14 ± 1 PSIG

Lubrication System

Oil Specification.....MIL-L-7808 at -54° to 54°C
(-65° to 130°F)

Oil Pressure.....75 to 105 PSIG

Oil Temperature.....65°C (150°F) Above Inlet

Electrical System

Power Supply.....26 ± 2V DC

Bleed Air Control System

Air Pressure Regulator.....39 IN. HG Gage (APPROX)

Unloading Air Shutoff Valve

Normal Position.....Closed

Bleed-Load Control Thermostat Temperature

Setting.....628°C (1165:F) (MAX)

Overall Dimensions

Height.....25.5 IN. (APPROX)

Length.....37.8 IN. (APPROX)

Width.....28.5 IN. (APPROX)

Unit Dry Weight.....250 LB. (APPROX)



TABLE II
VEHICLE DIMENSIONS

Item	Dimension
Cushion Length	7.92 ft
Cushion Beam	3.64 ft
Cushion Area	25.7 ft ²
Cushion Pressure	32.6 lb/ft ²
Total Pressure, Air Supply	6740 lb/ft ²
Air Density (at nozzle)	0.002305 slug/ft ³
Daylight Gap	0.495 ft
Equivalent Diameter	5.74 ft
Cushion Perimeter	20.5 ft
Daylight Gap Area	10.17 ft ²
Peripheral Jet Efflux Angle	30°
Nozzle Thickness	0.456 in
Total Air Flow Rate (Volume) (at nozzle)	20.3 ft ³ /sec
Cushion Discharge Coefficient	0.327 ft ²

TABLE III
STRUCTURAL WEIGHTS

Component	Area (ft ²)	Weight
Outer Hull	37.65	15.12
Inner Hull	34.43	13.83
Cushion Interior	27.74	11.16
Interior Spoilers	1.88	0.76
Total		40.87

TABLE IV

WEIGHTS OF OTHER STRUCTURAL MEMBERS AND ACCESSORIES

Component	Weight (lb)
Engine	217.00
Driver	180.00
Propeller and Gearing	150.00
Instrument Panel and Bracing	12.25
Engine Bracing	2.83
Elevator Mount	11.86
Control Column and Rudder Pedals	3.39
Pilot Seat	2.66
Main Structural Braces	26.40
Elevator and Rudder Pivot Post	4.32
Propeller Shroud	16.50
Fuel Tank	9.05
Fuel (35 gal. at 6.7 lb/gal)	234.00
Elevator and Rudder	6.30
Control Cables	0.10
Battery	100.00
Total	976.66

TABLE V
ESTIMATED PITCHING MOMENTS

Component	Lever Arm (ft)	Estimated Pitching Moment (ft-lb) (+ CW, - CCW)
Instrument Panel	4.67	-58.3
Control Column and Rudder Pedals	4.17	-14.1
Pilot and Seat	2.33	-426.
Engine	0.083	-18.1
Fuel and Fuel Tank	0.5	-121.5
Battery	1.83	+183.
Shroud	2.08	+34.4
Propeller and Gear	2.33	+350.
Elevator Mount	3.33	+39.5
Elevator and Rudder Pivot Posts	3.33	+14.4
Elevator and Rudder	3.58	+22.6
Total		+5.9

TABLE VI
PROPELLER PERFORMANCE ESTIMATION

Item No.	Power Setting →	1	2	3	4	5	6	7
1	DIAMETER	4	4	4	4	4	4	4
2	TAF	600	600	600	600	600	600	600
3	C_{Li}	0.5	0.5	0.5	0.5	0.5	0.5	0.5
4	A_4/A_2	1.2	1.2	1.2	1.2	1.2	1.2	1.2
5	ATTITUDE	Hover	Hover	Creep	Creep	Creep	Creep	Creep
6	BHP	50	60	70	80	75	90	100
7	ENGINE RPM	6000	6000	6000	6000	6000	6000	6000
8	ALTITUDE	S.L	S.L	S.L	S.L	S.L	S.L	S.L
9	V_{ok}	0	0	20	20	20	30	30
10	ρ_{SL}/ρ_0	1	1	1	1	1	1	1
11	f_c	1	1	1	1	1	1	1
12	N	2700	2700	2700	2700	2700	2700	2700
13	M_0	0	0	0.0302	0.0302	0.0302	0.0453	0.0453
14	$ND_p \times f_e$	10,800	10,800	10,800	10,800	10,800	10,800	10,800
15	C_p	0.1245	0.1494	0.1743	0.1992	0.1867	0.2241	0.2490
16	J_0	0	0	0.1877	0.1877	0.1877	0.2816	0.2816
17	J_0/J_2	0	0	0.2108	0.2018	0.2062	0.2858	0.2774
18	J_2	0.775	0.825	0.890	0.930	9.910	9.985	1.015
19	$J_2 \text{ max}$	>4	>4	>4	>4	>4	>4	>4
20	V_{2k}	82.5	87.9	94.8	99.0	96.9	104.9	108.1
21	η_{oT}	----	----	39.0	36.5	37.5	48.0	46.5
22	C_{TT}/C_p	2.85	2.69	----	----	----	----	----
23	T_T	435.4	493.2	445.0	475.9	458.4	469.4	505.3

PROPELLER PERFORMANCE ESTIMATION

24	A_2	11.42	11.42	11.42	11.42	11.42	11.42	11.42
25	T_T/A_2	38.11	43.17	38.95	41.66	40.13	41.09	44.23
26	F_D	0.955	0.960	0.950	0.950	0.950	0.950	0.950
27	η_{oTE}	----	----	37.0	34.7	35.6	45.6	44.2
28	C_{TTE}/C_p	2.72	2.58	----	----	----	----	----
29	T_{TE}	415.8	473.5	422.7	452.2	435.5	446.0	480.0
30	$\theta_{3/4}$	20.0	21.7	23.	25.0	24.2	26.5	27.8
31	J_o/J_2 ideal	0	0	0.2094	0.2009	0.2046	0.2816	0.2733
32	η_{oT} ideal	----	----	39.0	39.0	39'0	49'5	46.5
33	C_{TT}/C_p ideal	2.95	2.77	----	----	----	----	----
34	T_T ideal	450.7	507.8	445.0	482.5	464.6	474.3	505.3
35	J_2 ideal	0.795	0.840	0.896	0.934	0.917	1.000	1.030
36	V_2 ideal	84.67	89.47	95.43	99.48	97.67	106.51	109.70
37	$A_2/A_4+J_o/J_2$	----	----	1.0441	1.0351	1.0395	1.1191	1.1107
38	η_{oP}	----	----	20.36	18.89	19.49	26.86	25.82
39	C_{TP}/C_p	1.19	1.12	----	----	----	----	----
40	T_P	181.4	205.5	232.5	246.5	238.0	262.7	280.6
41	η_{2P}	92.3	92.5	96.5	93.7	94.7	94.1	93.2
42	$A_2/A_4+J_o/J_2i$	----	----	1.0427	1.0342	1.0379	1.1149	1.1066
43	η_{oP} ideal	----	----	20.3	19.1	19.7	27.0	25.9
44	C_{TP}/C_p ideal	1.23	1.15	----	----	----	----	----
45	T_P ideal	187.8	211.5	232.5	249.5	236.0	264.0	279.3
46	η_{2P} ideal	97.8	96.6	97.0	95.0	96.3	95.9	95.0

TABLE VII
PROPELLER SELECTION CRITERIA

VELOCITY, KNOTS	0	20	30
Propeller Characteristics (TAF/C _{1i} /N)	η_{2p}	η_{2p}	η_{2p}
1000/0.3/3000	93.0	86.8	89.3
600/0.5/2700	92.9	91.4	94.5
800/0.15/3000	92.7	92.0	90.7
400/0.5/3000	92.3	89.7	94.2
800/0.5/2700	92.7	92.8	93.4
600/0.3/3000	91.2	92.0	91.7

TABLE VIII
YAW CONTROL DATA

α_{or}	c_l	α_{ir} (Deg)	α_{er}	C_{Lr}	L	N
0	0	0	0	0	0	0
1	0.10	0.533	0.467	0.0467	4.14	14.4
2	0.20	1.065	0.935	0.0935	8.29	29.0
3	0.30	1.598	1.402	0.1402	12.43	43.5
4	0.41	2.18	1.720	0.172	15.25	43.4
5	0.51	2.72	2.28	0.228	20.2	70.7
6	0.63	3.36	2.64	0.264	23.4	81.9
7	0.72	3.83	3.17	0.317	28.1	98.4
8	0.85	4.52	3.48	0.348	30.9	118.0
9	0.92	4.90	4.10	0.420	37.2	130.0
10	1.05	5.60	4.40	0.450	39.9	139.5
11	1.15	6.13	4.87	0.497	44.0	154.0
12	1.25	6.67	5.33	0.543	48.2	168.5

TABLE IX

PITCH CONTROL DATA

α_{oe}	C_l	α_{ie}	α_{ee}	C_{Le}	(2 L sections)	M
0	0	0	0	0	0	0
1	0.10	0.594	0.406	0.04	1.586	5.35
2	0.20	1.184	0.816	0.08	3.17	10.70
3	0.30	1.779	1.221	0.122	4.84	16.34
4	0.41	2.44	1.56	0.156	6.18	20.9
5	0.51	3.03	1.97	0.197	7.80	26.3
6	0.63	3.76	2.24	0.224	8.88	30.0
7	0.72	4.28	2.72	0.272	10.78	36.4
8	0.85	5.06	2.94	0.294	11.66	39.4
9	0.92	5.47	3.53	0.353	14.00	47.2
10	1.05	6.37	3.63	0.363	14.40	48.6
11	1.15	6.86	4.14	0.414	16.40	55.3
12	1.25	7.46	4.54	0.454	17.98	60.6

TABLE X
THROTTLING ALTERED PARAMETERS

Parameter	Value (Throttled)
S_N'	0.710 ft ²
P_N'	2085 lb/ft ²
V_j'	389 ft/sec
x' (for section with throttle activated)	0.0598
$\Delta p'$	36.0 lb/ft ²
C_j' (for section with throttle activated)	17.32
Θ'	23.5°
t' (for section with throttle activated)	0.0416 ft

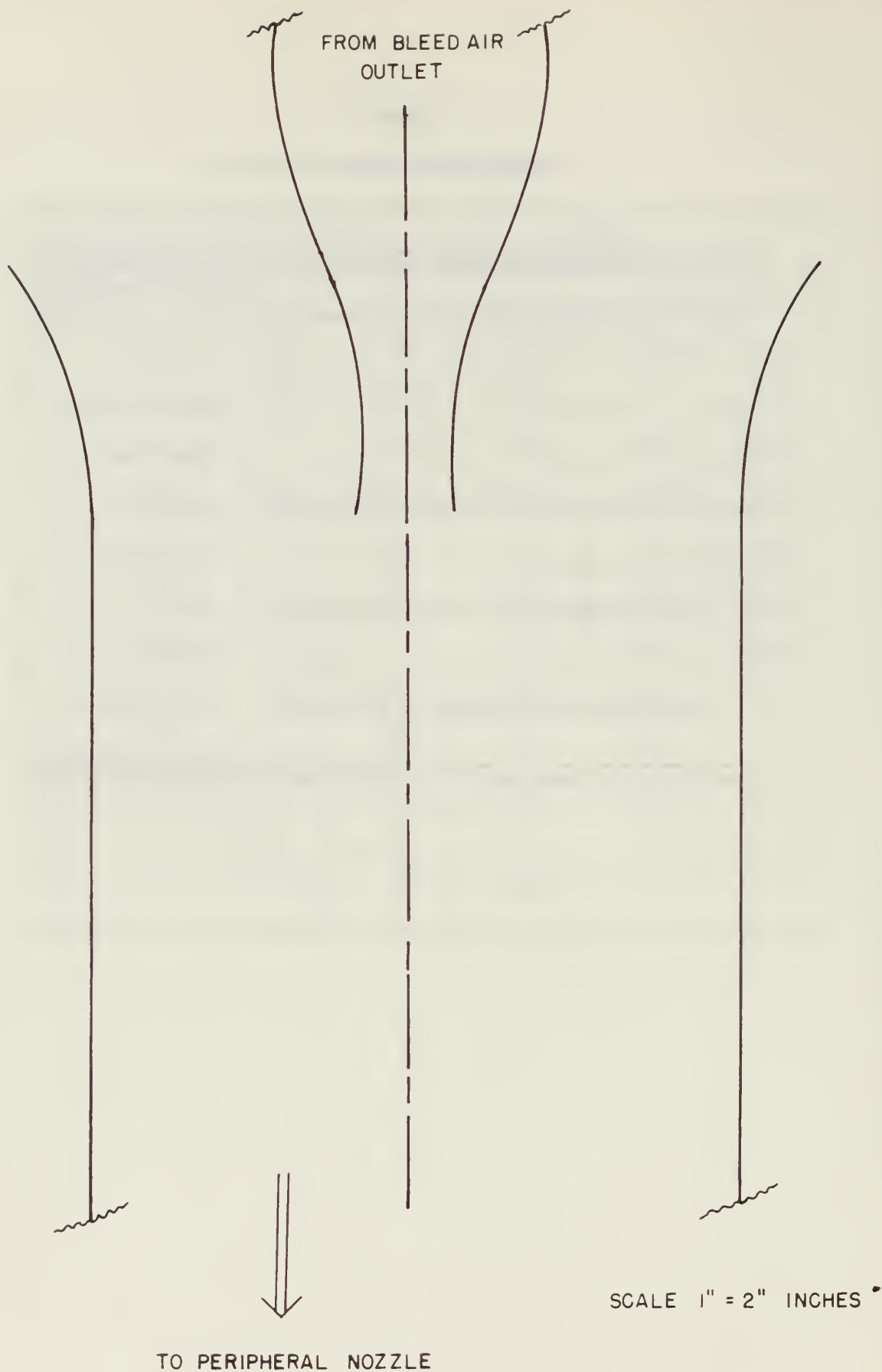
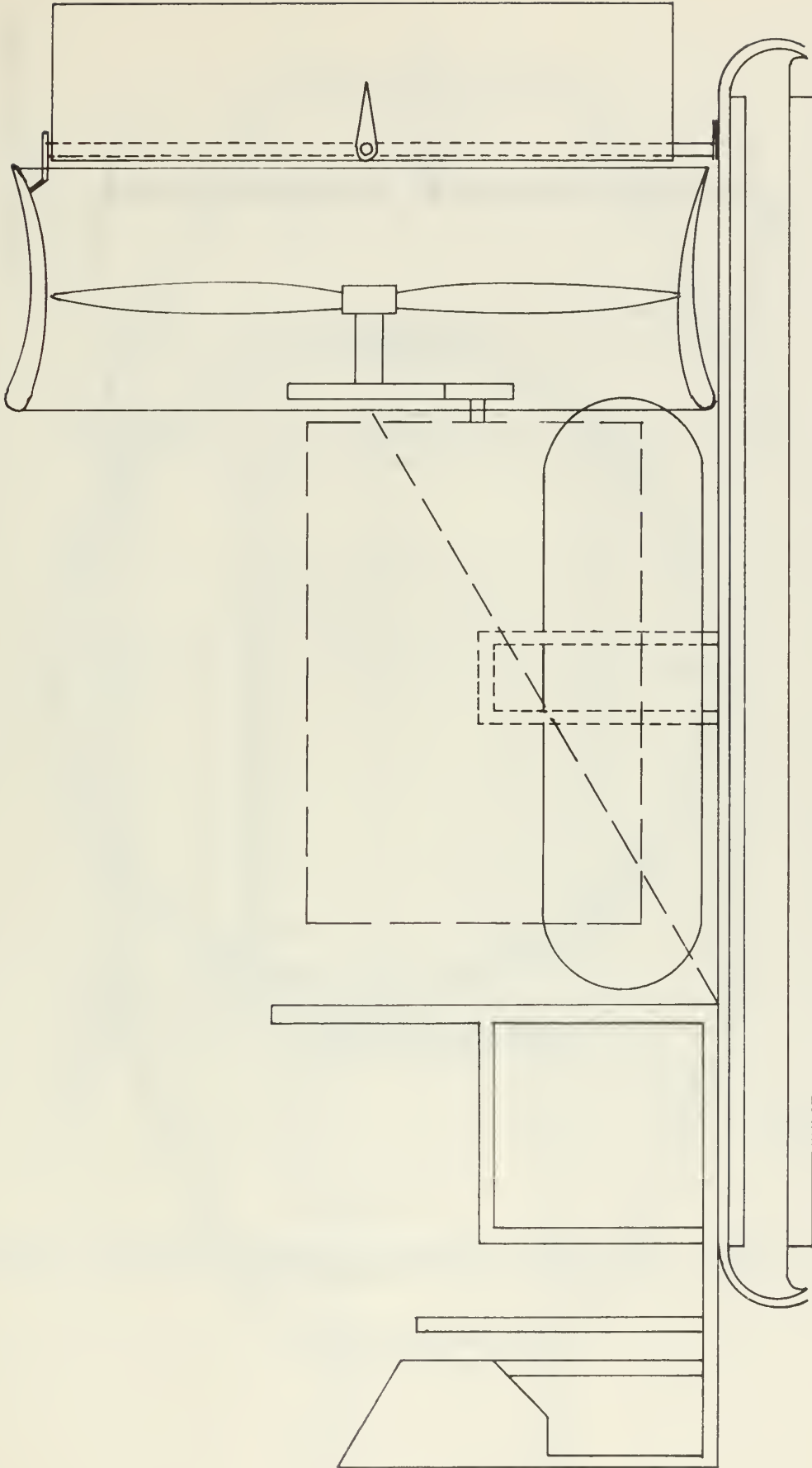


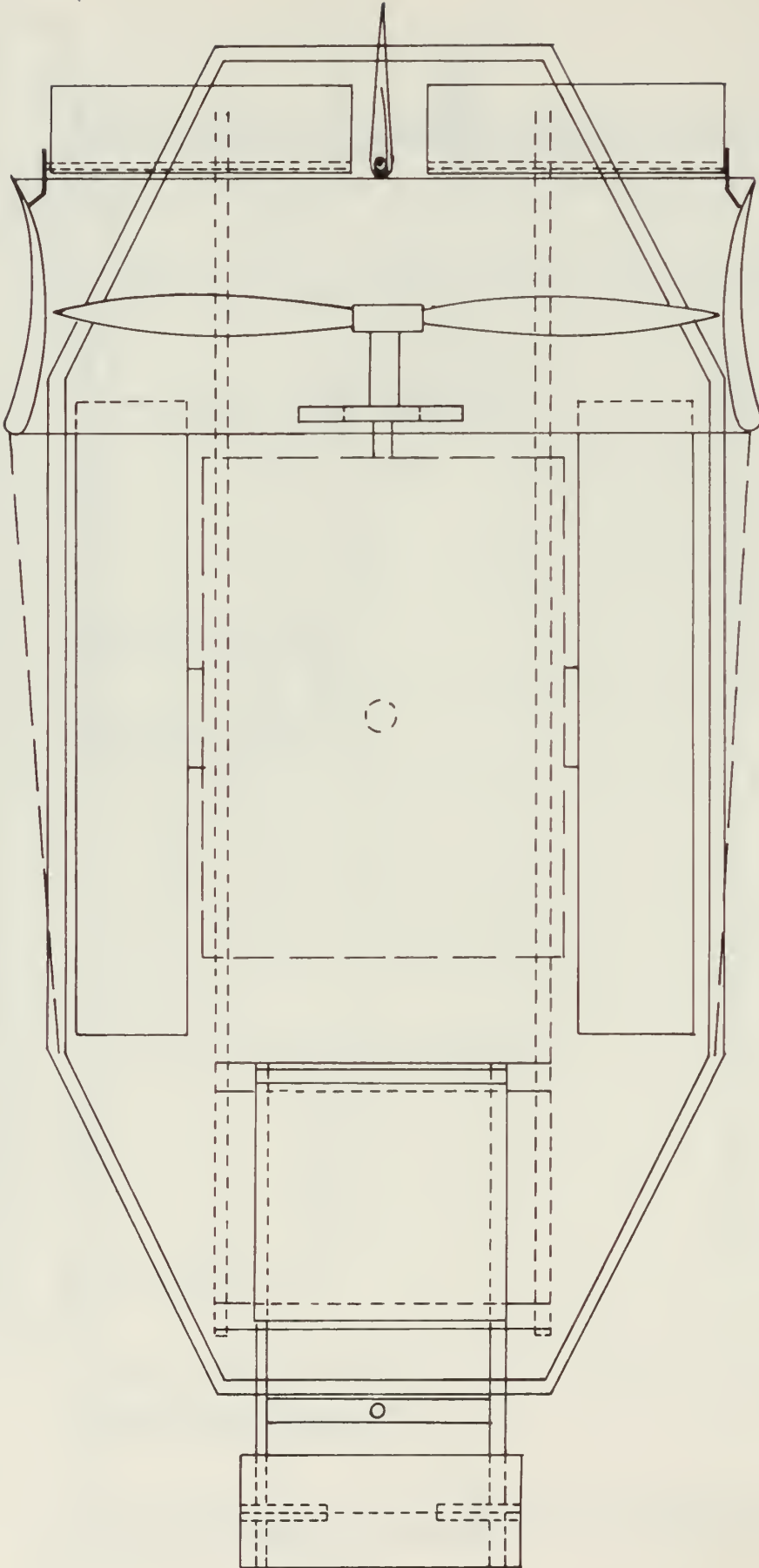
FIG 1. BLEED AIR DUCTING INCLUDING CONVERGING-DIVERGING NOZZLE



SCALE 1:12 INCHES

FIG 2.

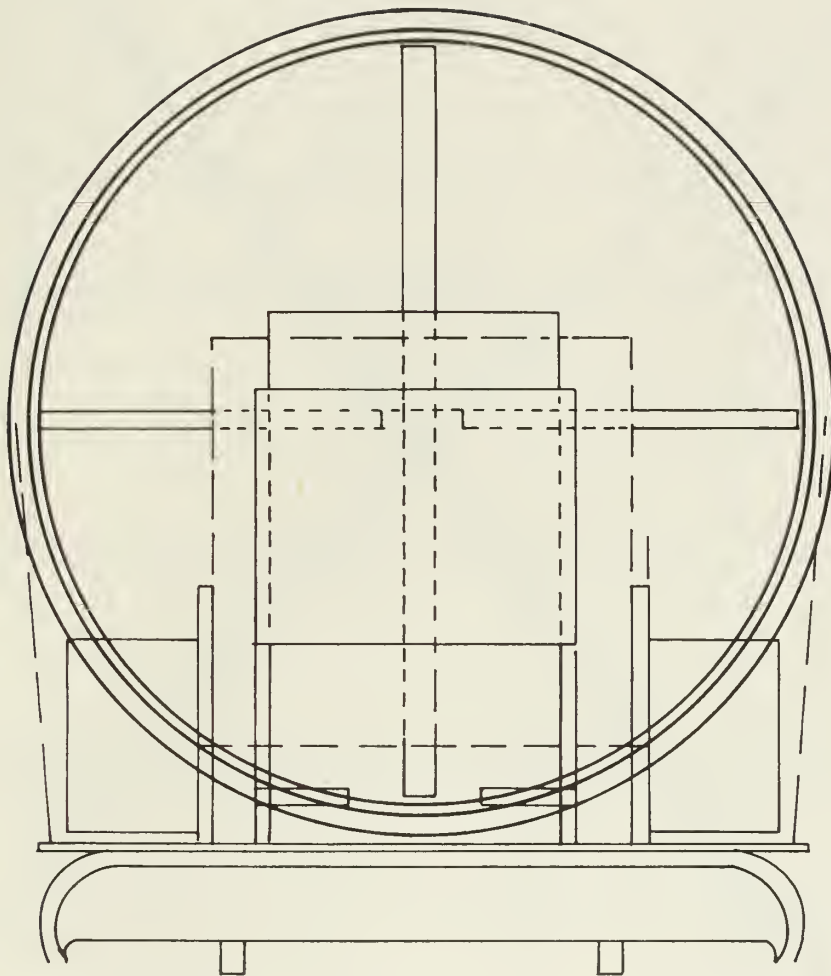
LEFT SIDE VIEW OF GROUND EFFECT MACHINE, FINAL DESIGN



SCALE 1:12 INCHES

FIG 3.

TOP VIEW OF GROUND EFFECT MACHINE, FINAL DESIGN



SCALE 1:12
INCHES

FIG 4.

FRONT VIEW OF GROUND EFFECT MACHINE , FINAL DESIGN

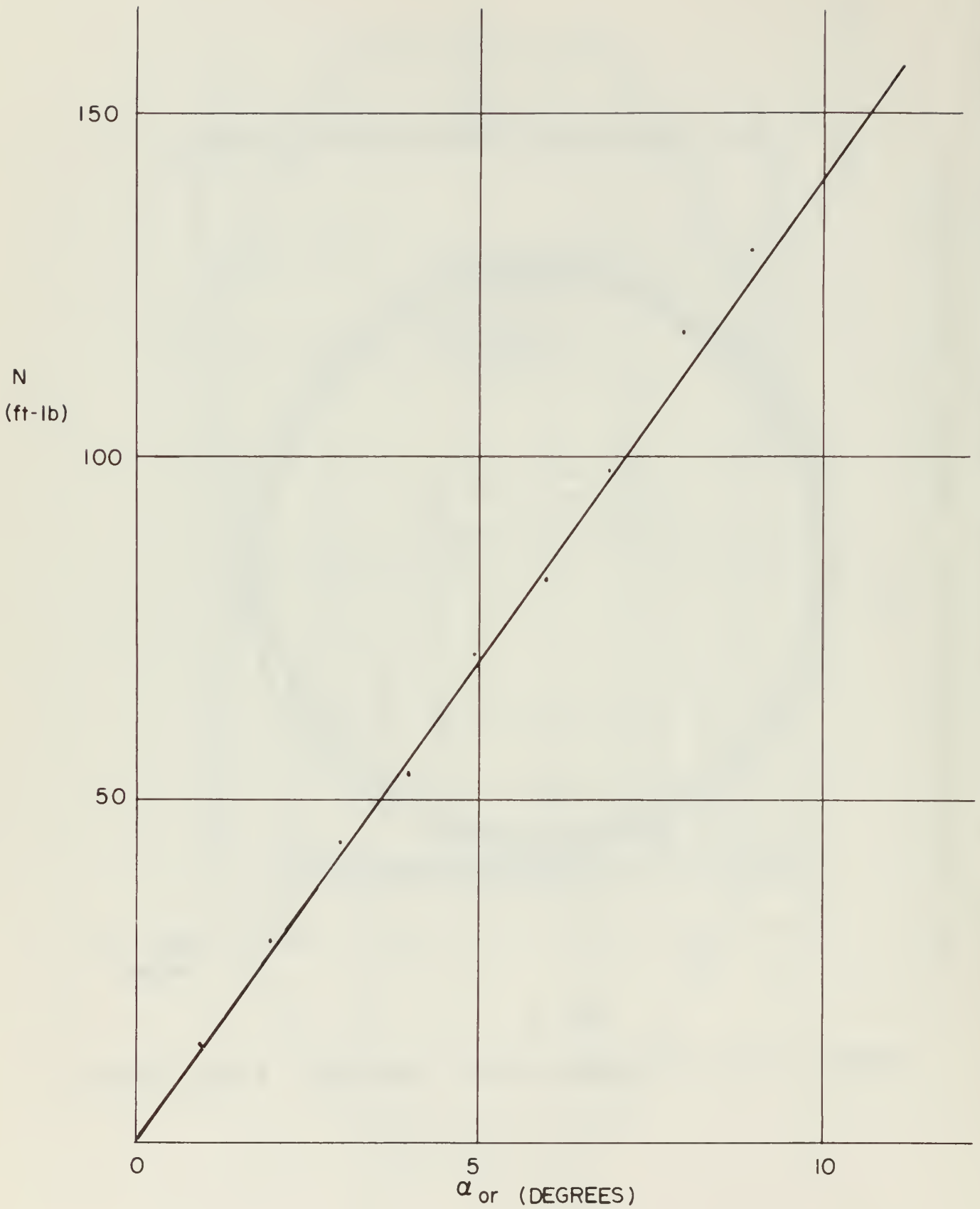


FIG 5.

RUDDER CONTROL MOMENT vs RUDDER DEFLECTION ANGLE

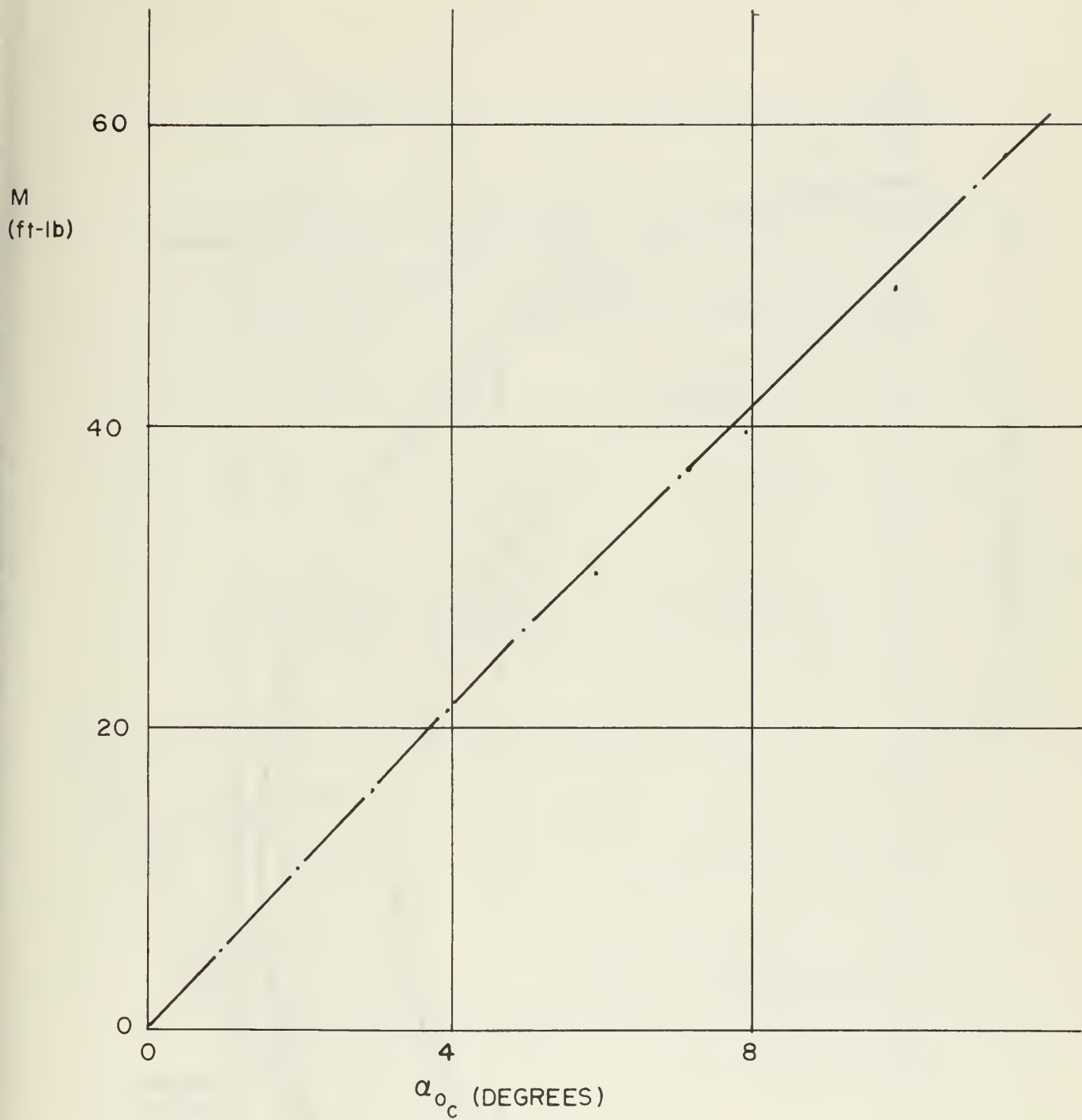


FIG 6.

ELEVATOR CONTROL MOMENT vs ELEVATOR DEFLECTION ANGLE

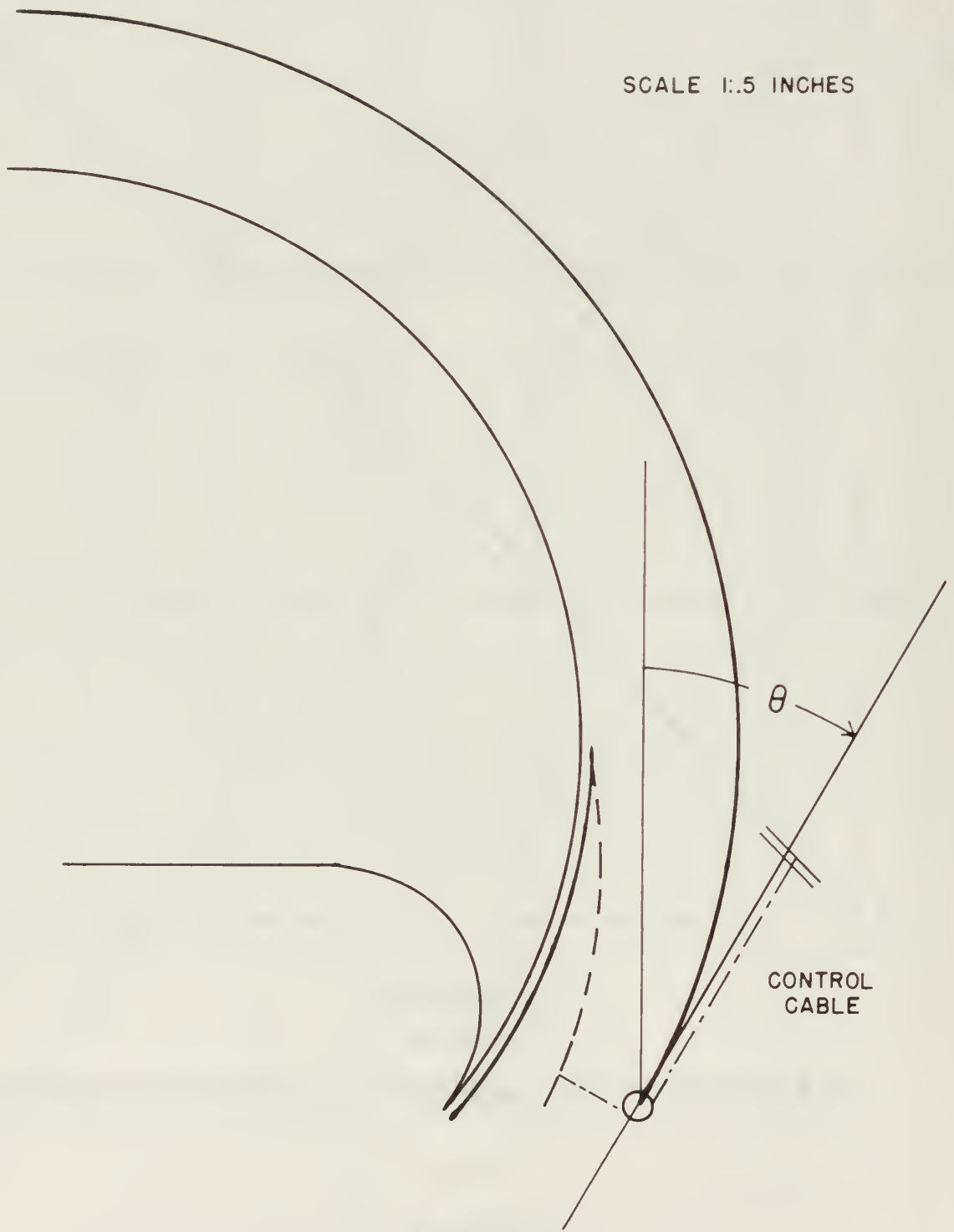


FIG 7. THROTTLE MECHANISM

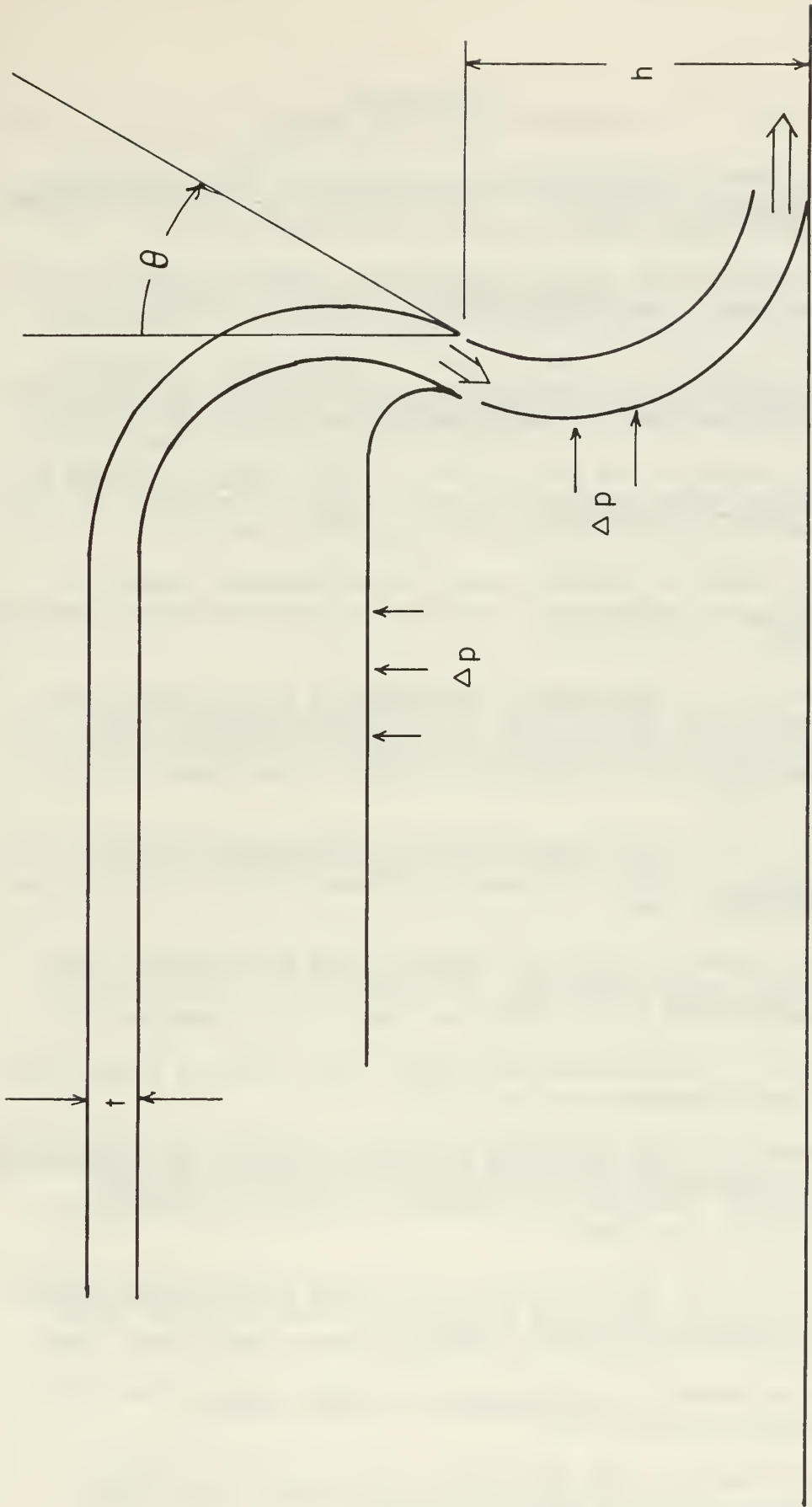


FIG 8. ORIENTATION OF θ , t , AND h

BIBLIOGRAPHY

- Burgan, Elmer T., Wind-Tunnel Investigation of DTMB Rectangular Planform GEM Model 472. Washington, D. C.: David Taylor Model Basin, Report 1644, Aero Report 1026, May 1962.
- Campbell, John Paul, Vertical Takeoff and Landing Aircraft. New York: The MacMillan Company, 1962.
- Chaplin, Harvey R. and Ford, Allen G., Some Design Principles of Ground Effect Machines Section B - Air Cushion Mechanics. Washington, D. C.: David Taylor Model Basin, 1966.
- Chaplin, Harvey R. and Ford, Allen G., Some Design Principles of Ground Effect Machines Section D - Drag. Washington, D. C.: David Taylor Model Basin, Report 2121D, June 1966.
- Dommasch, Daniel O., Sherby, Sydney S. and Connolly, Thomas F., Airplane Aerodynamics. New York: Pitman Publishing Corporation, 1951.
- Fink, Martin D., Experimental Investigation of the Effects of Stabilizing Nozzle Width on the Hovering Stability and Performance of a Circular GEM Model. Washington, D. C.: David Taylor Model Basin, Report 1711, Aero Report 1047, Feb. 1963.
- Hackett, J. E., Wind Tunnel Tests of a Streamlined Fan-Lift Nacelle. London: Aeronautical Research Council Reports and Memoranda, 1967.
- Johnson, Arthur E., Phase II Tethered Tests and Low-Speed Free Flight Tests of GEM III. Washington, D. C.: David Taylor Model Basin, Report 1700, Aero Report 1049, December 1962.
- Kohler, H. L., Unpublished Low Speed Flight Mechanics Class Notes. Naval Postgraduate School, 1967.
- Kurylowich, G., The Light-Line Tethering Technique for Determining the Aerodynamic Derivatives of an Air Cushion Vehicle. Toronto: Institute for Aerospace Studies of University of Toronto, Sept. 1965.
- Lester, W. G. S. and Kiernan, F. T., A Note on Some Static Tests of Flexible Skirts for Hovercraft. Great Britain: Royal Aircraft Establishment, Technical Report 66053, Feb. 1966.
- McCormick, Barnes W., Aerodynamics of V/STOL Flight. New York: Academic Press, 1967.
- Miller, Richard A., The Development and Testing of a Control Decoupler for Air Cushion Vehicles. Groton, Connecticut: General Dynamics, Oct. 1966.

- Nelson, Wilbur C., Airplane Propeller Principles. New York:
John Wiley and Sons, Inc., 1944.
- Ramsden, J. M. (ed.), "Air-Cushion Vehicles," Flight International,
Oct. 1967, pp. 46-58.
- Tinajero, Anibal Alfredo, A Preliminary Design Technique for
Plenum-Chamber Ground Effect Machines (GEM's). Washington, D. C.:
David Taylor Model Basin, Report 1621, Aero Report 982, June 1960.
- U. S. Naval Air Development Center, Captured Air Bubble (CAB)
High-Speed Over-Water Vehicle Report. Johnsville, Pa.:
Department of the Navy, May 1964.

REFERENCES

1. Lambert, John L., Air Cushion Vehicle Mass Transportation Demonstration Project -- CAL-MTD-3 Oakland, California: Port of Oakland, 1967, p. 59.
2. Chaplin, Harvey R., Ground Effect Machine Research and Development in the United States, Washington, D. C.: David Taylor Model Basin, Report 1463, Aero Report 994, Dec. 1960.
3. Operation and Maintenance Instructions - Pneumatic and Shaft Power Gas Turbine Engine - Report No. 6A-144 (2). Phoenix, The Garrett Corporation AirResearch Manufacturing Division, 1962.
4. Armfield, William J., IV, et al., Air Cushion Vehicles Transportation of the Future. New York: Transportation Research Associates, 1962.
5. Croome, Angela, Hover Craft. Leicester: Brockhampton Press Ltd., 1962.
6. Chaplin, Harvey R. and Ford, Allen G., Some Design Principles of Ground Effect Machines Section A - Introductory Survey Washington, D. C.: David Taylor Model Basin, Report 2121A, April 1966.
7. Generalized Method of Shrouded Propeller Performance Estimation. Windsor Locks, Connecticut: Hamilton Standard Division of United Aircraft Corporation.
8. Shapiro, Ascher H., The Dynamics and Thermodynamics of Compressible Fluid Flow. New York: The Ronald Press Company, 1954.
9. Eshbach, Ovid W., Handbook of Engineering Fundamentals. New York: John Wiley & Sons, Inc., 1952.
10. Chaplin, Harvey R. and Ford, Allen G., Some Design Principles of Ground Effect Machines Section D - Drag. Washington, D. C.: David Taylor Model Basin, Report 2121D, June 1966.

APPENDIX A

DERIVATION OF CERTAIN FORMULAS

Equation II-1 (Ref. 2)

See Figure 1.

The sum of the forces acting on the stream of air from the peripheral jet per unit periphery is equal to the change in momentum, per unit periphery, of that stream of air:

$$\frac{\sum F}{C} = \frac{\dot{m}}{C} (V_j - V_2)$$

C = cushion periphery

V_2 = final velocity of the air stream

$$= -V_j (\sin \Theta)$$

It is assumed that only the direction of flow changes (that is, the speed remains constant). See Fig. 7 for the orientation of the angle Θ . The only force acting on the air stream is the cushion pressure, Δp , acting over the daylight clearance, h , around the periphery C .

Thus

$$\frac{\sum F}{C} = \Delta p h$$

Also

$$\dot{m} = \rho_N S_g V_j$$

so that

$$\frac{\dot{m}}{C} = \frac{\rho_N S_g V_j}{C}$$

but

$$S_g = hC$$

Therefore substitution yields

$$\begin{aligned} \Delta p h &= \rho_N t V_j (V_j + V_j \sin \Theta) \\ &= \rho_N t V_j^2 (1 + \sin \Theta) \end{aligned}$$

Equation II-2

The volume flow rate out of the peripheral jet is the product of the velocity of air out of the jet, V_j , times the total area it traverses, $S_N = tC$

where

t = nozzle thickness

C = nozzle perimeter

The compressor pressure rise is equal to the jet total pressure and is the sum of the mean dynamic pressure (approximated by $1/2 \rho_N V_j^2$) and the mean static pressure (approximated by $1/2 \Delta p$). The power required is then the product of the jet volume flow rate times the compressor pressure rise:

$$P_c = V_j t C (1/2 \rho_N V_j^2 + 1/2 \Delta p)$$

APPENDIX B

SOLUTION OF CONVERGING-DIVERGING NOZZLE EXIT PRESSURE

See Figure 8.

Having chosen an outer pipe area, utilization of the continuity, energy, momentum, and state equations as well as the assumption of adiabatic mixing in the outer pipe downstream of the nozzle allows the solution of the flow properties through the bypass area and at station 3, the outer pipe exit. These equations are as follows:

Continuity

$$\underline{\dot{m}_b} + \dot{m}_2 = \underline{\dot{m}_3} \quad \text{B1}$$

Energy

$$2gJC_p(\dot{m}_2 T_2 + \underline{\rho_a A_b V_b T_b} - \underline{\rho_a A_3 V_3 T_3}) = \underline{\rho_3 A_3 V_3^3} - \dot{m}_2 V_2^2 - \underline{\rho_a A_b V_b^3} \quad \text{B2}$$

Momentum

$$\begin{aligned} p_2 A_2 - p_3 A_3 &= \underline{\dot{m}_3 V_3} - \dot{m}_2 V_2 - \underline{\dot{m}_b V_b} \\ &= \underline{\rho_3 A_3 V_3^2} - \dot{m}_2 V_2 - \underline{\rho_b A_b V_b^2} \end{aligned} \quad \text{B3}$$

State

$$\underline{\rho_3} = \underline{p_3} / \underline{RT_3} \quad \text{B4}$$

Adiabatic Mixing

$$\underline{T_3} = \frac{\dot{m}_2 T_2 + \underline{\rho_b A_b V_b T_b}}{\underline{\rho_b A_b V_b} + \dot{m}_2} \quad \text{B5}$$

where the underlined variables are the unknowns for which a solution is desired.

Assuming ρ_b and T_b to be standard atmospheric conditions and defining the mass flow rate ratio, X , as

$$X = \frac{\underline{\dot{m}_b}}{\dot{m}_2}$$

the equations can be rewritten as

$$\frac{\dot{m}_3}{\dot{m}_2} = (1 + X) \quad \text{B1'}$$

$$p_2 A_2 - p_3 A_3 = \dot{m}_2 \left[(1 + X)v_3 - v_2 - Xv_b \right] \quad \text{B3'}$$

$$0 = (1 + X) v_3^2 - v_2^2 - Xv_b^2 \quad \text{B2'}$$

$$\rho_3 = p_3 / RT_3 \quad \text{B4}$$

$$T_3 = (T_2 + XT_b) / (X + 1) \quad \text{B5'}$$

Now defining

$$C = \rho_b A_b / \rho_2 A_2 v_2$$

these equations can then be combined to yield

$$\frac{p_2 A_3}{\dot{m}_2} - \frac{gR(T_2 + XT_b)}{\left(\frac{v_2^2 + X^3/C^2}{1 + X} \right)^{1/2}} = (1 + X) \left(\frac{v_2^2 + X^3/C^2}{1 + X} \right)^{1/2} - v_2 - \frac{X^2}{C}$$

which can be solved numerically for X if a specific value of p_2 is assumed. From this value of X, a value for M_b , the Mach number of the bypass air, can be found and then compared with the value of M_b computed from the pressure ratio p_b/p_{ob} where p_{ob} is assumed to be atmospheric. Various values of p_2 can be tried until the two values of M_b match. When this occurs, the correct value of p_2 for the given A_3 has been found.

INITIAL DISTRIBUTION LIST

	No. Copies
1. Defense Documentation Center Cameron Station Alexandria, Virginia 22314	20
2. Library Naval Postgraduate School Monterey, California 93940	2
3. Commander, Naval Air Systems Command Navy Department Washington, D. C. 20360	1
4. Professor H. L. Kohler Department of Aeronautics Naval Postgraduate School Monterey, California 93940	1
5. Chairman, Department of Aeronautics Naval Postgraduate School Monterey, California 93940	1
6. Professor A. E. Fuhs Department of Aeronautics Naval Postgraduate School Monterey, California 93940	1
7. LT Martin Peck Merrick, USN 4304 Arthur Avenue Brookfield, Illinois 60513	1
8. Dr. Harvey R. Chaplin Naval Ship Research and Development Center Washington, D. C. 20007	1

DOCUMENT CONTROL DATA - R&D

(Security classification of title; body of abstract and indexing annotation must be entered when the overall report is classified)

1. ORIGINATING ACTIVITY (Corporate author) Naval Postgraduate School Monterey, California 93940		2a. REPORT SECURITY CLASSIFICATION Unclassified	
		2b. GROUP	
3. REPORT TITLE A PRELIMINARY DESIGN STUDY FOR A GROUND EFFECT MACHINE			
4. DESCRIPTIVE NOTES (Type of report and inclusive dates)			
5. AUTHOR(S) (Last name, first name, initial) Martin Peck Merrick Lieutenant, U. S. Navy			
6. REPORT DATE March 1968		7a. TOTAL NO. OF PAGES 65	7b. NO. OF REFS 10
8a. CONTRACT OR GRANT NO.		9a. ORIGINATOR'S REPORT NUMBER(S)	
b. PROJECT NO.			
c.		9b. OTHER REPORT NO(S) (Any other numbers that may be assigned this report)	
d. <i>Unlimited dist</i>			
10. AVAILABILITY/LIMITATION NOTICES This document is subject to special export controls and each transmittal to foreign governments or foreign nationals may be made only with prior approval of the Department of the Navy.			
11. SUPPLEMENTARY NOTES		12. SPONSORING MILITARY ACTIVITY Naval Postgraduate School Monterey, California 93940	
13. ABSTRACT This paper provides the results of a preliminary design study of a ground effect machine to be built at the Naval Postgraduate School, Monterey, California. The design is based on an engine currently available at the School and covers such factors as lift versus weight, thrust versus drag, balance, stability, control, and instrumentation. The final design chosen was a peripheral jet type ground effect machine with a cushion area of 25.7 square feet, driven by a 4 foot diameter shrouded propeller. Total engine power of 203 horsepower is sufficient to provide 1017 pounds of lift at a hover height of 5.95 inches and 446 pounds of thrust at 30 knots.			

14

KEY WORDS

LINK A

LINK B

LINK C

ROLE

WT

ROLE

WT

ROLE

WT

Ground Cushion
 Air Curtain Vehicle
 Peripheral Jet



NO FOR

thesM535

A preliminary design study for a ground



3 2768 001 88617 9

DUDLEY KNOX LIBRARY